

# Study on Discontinuity Properties of Phased-Array Ultrasound Transducer Affecting to Sound Pressure Fields Pattern

Tran Trong Thang, Nguyen Phan Kien, Trinh Quang Duc

**Abstract**—The phased-array ultrasound transducer types are utilities for medical ultrasonography as well as optical imaging. However, their discontinuity characteristic limits the applications due to the artifacts contaminated into the reconstructed images. Because of the effects of the ultrasound pressure field pattern to the echo ultrasonic waves as well as the optical modulated signal, the side lobes of the focused ultrasound beam induced by discontinuity of the phased-array ultrasound transducer might be the reason of the artifacts. In this paper, a simple method in approach of numerical simulation was used to investigate the limitation of discontinuity of the elements in phased-array ultrasound transducer and their effects to the ultrasound pressure field. Take into account the change of ultrasound pressure field patterns in the conditions of variation of the pitches between elements of the phased-array ultrasound transducer, the appropriated parameters for phased-array ultrasound transducer design were asserted quantitatively.

**Keywords**—Phased-array ultrasound transducer, sound pressure pattern, discontinuous sound field, numerical visualization.

## I. INTRODUCTION

ULTRASOUND is physical energy being a useful tool for optical modulation in biomedical applications such as optical imaging and spectroscopy [1]-[6]. Since the sizes of the acoustic scattering particles presenting in biological tissues typically are ranged in few tens micrometers [7], the acoustic scattering of the ultrasonic waves in biological tissues is low, leading to maintain of spatial information of the biological objects in biological tissues. Therefore, the ultrasound field can be used as a utility to extract the chemical, optical as well as the spatial information of the biological objects by modulation of the light propagated in the biological tissues. Since the modulation of the light for optical imaging based on the acousto-optic effect, the characteristics of the modulated signal mainly depends on the acoustic pressure field especially is focused pressure field [11].

However, according to a development using phased-array ultrasound transducer to modulate the fluorescence [8], [9], the fluorescence position in obtained images are not correspondent to the localized fluorescence position in biological tissues because of the discontinuity of the phased-

array transducer. This phenomenon did not occur in the case of which the modulation was performed by a single element ultrasound transducer [10].

To clarify the physical effects, a numerical method was employed to investigate the pattern of ultrasound pressure field under consideration of variation of the pitch between each elements of the phased-array ultrasound transducer. With visualization of the sound pressure field through computational simulation of interference induced from the acoustic emission of the ultrasound elements, the parameters of relationship between the pitch of each element and their frequency oscillation influencing to the pattern of the sound pressure field will be figured out and asserted.

For this purpose, in this paper, the ultrasound transducer considered as a concave transducer with elements arranged as array lining in the surface of the phased-array ultrasound transducer. By the algorithm of wave superposition calculation at positions in a plane, the 2D image of ultrasound pressure field can be reconstructed. Under variation of the pitch in condition of a constant acoustic frequency, the sound pressure field of the phased-array ultrasound transducer will be analyzed and evaluated throughout the pattern of the sound pressure field.

## II. THEORETICAL APPROACHES

The phased-array transducers were designed as arrays of piezoelectric elements arranged in a geometrical surface such as 1D rectangular linear, 2D rectangle, 3D sphere, ring, and cone usually and the beam forming of the ultrasound field generated through these phased-array ultrasound transducer can be regulated with an array of driven waves initial phases so called “phased-array”.

For the optical imaging using acousto-optic modulation, the required ultrasound beams are focused ultrasound field since the sound pressure values at the focal region of the ultrasound beam are distinguished, thus the light modulated signal and the position of focal point provide intensity and their spatial information for the optical image. Because of the discontinuity of the phased-array ultrasound transducer just influence to the acoustic field but not depends on the ultrasound types as well as driven waves, hence, to simplify the investigated circumstances, the calculation for the driven wave initial phases are neglected and the focused ultrasound beam can be considered as the generation of sinusoidal wave from a 3D concave spherical phased-array ultrasound transducer instead.

Tran Trong Thang is with the Electronic & Telecommunication of Faculty, Electric Power University, Ha Noi, Viet Nam (e-mail: thangtt@epu.edu.vn).

Nguyen Phan Kien and Trinh Quang Duc are with the Biomedical Engineering Department, Ha Noi University of Science and Technology, Ha Noi, Viet Nam (e-mail: kien.nguyenphan@hust.edu.vn, duc.trinhquang@hust.edu.vn).

Assuming that the ultrasound pressure at a point in space is superposed from the waves emitted by piezoelectric elements distributed uniformly on the spherical dome surface and each element driven by the same electrical sinusoidal wave to generate the same acoustic sinusoidal wave, the ultrasonic wave can be expressed as

$$P_i(t, r) = P_0 \sin(\omega t + Kr_i(x, y, z) + \varphi_i). \quad (1)$$

where the  $P_i$  is sound pressure of the element  $i$  at a time of,  $r_i$  is the distance from the element to a point in space,  $\omega$  is the angular frequency,  $K$  is the wave number, and  $P_0$  is the amplitude of the sound pressure.

Because of the elements array is arranged as spherical dome surface, the generated beam is focused on a point in space obeying the focal law [12] without the initial phase value, hence in this circumstance the  $\varphi_i$  can be simply assigned as 0. At a point in space in the condition of the same point of time, the synthesized wave can be considered as the sum of the waves generated by driven element at the point of time. The sound pressure at the point in space is simply written as

$$P_r = \sum_{i=1}^n P_i(t, r) = \sum_{i=1}^n P_0(\omega t + kr_i(x, y, z)). \quad (2)$$

As shown in (2), the sound pressure presenting in a point depends on the arrays of distances from the phased-array ultrasound transducer elements to the point.

For a volume in space, each distance from a point space to a center of element in the phased-array ultrasound transducer can be presented easily by Pythagoras equation as

$$r_i(x, y, z) = \sqrt{(x_i - x_p)^2 + (y_i - y_p)^2 + (z_i - z_p)^2} \quad (3)$$

where the  $x_i, y_i, z_i$  are the coordinates of the element centers of the phased-array ultrasound transducer and  $x_p, y_p, z_p$  are the coordinates of the point in space. Therefore, if we insert (3) into (2) with a certain length of time, the amplitude of sound pressure at the point in space will be calculated. In the variation of the coordinates of the point in space the pattern of the sound pressure field can be visualized.

Since the ultrasound pressure field pattern can be observed by calculation of the sound pressure amplitude, therefore, under the variation of the pitch parameters between elements of the phased-array ultrasound transducer, the characteristics of the sound pressure field can be investigated and evaluated.

### III. THE NUMERICAL ALGORITHM

Based on (2), the pattern of ultrasound field pressure in a volume in space can be reconstructed numerically throughout calculation of the sound pressure with the number of derivative volumes. However, because of the computation cost and difficulties in rendering, this work reduced the calculation by the investigation the effects of pitch between elements of the phased-array ultrasound transducer to the ultrasound

pressure field pattern in a plane, which the  $z_i$  coordinates are neglected.

The pattern of the sound pressure distribution in this plane will characterize the sound pressure field distributed in space with assumption that the acoustic waves propagated as spherical waves in homogenous media. To discrete the spatial domain, the plane was divided to be a matrix with the positions of the matrix elements are correspondent to the  $x$  and  $y$  coordinates of the points in the plane, respectively. If  $m$  is the number of the rows and  $n$  is the number of the columns, the matrix can be expressed through the point as

$$M_{plane} = \begin{bmatrix} p_{1,1} & \cdots & p_{1,n} \\ \vdots & \ddots & \vdots \\ p_{m,1} & \cdots & p_{m,n} \end{bmatrix}. \quad (4)$$

where  $p_{j,k} = (x_j, y_k)$   $p_{j,k} = (x_j, y_k)$ . Therefore, for the distances from the piezoelectric elements center to the points in the plane, (2) can be rewritten as

$$r_{i,j,k} = \sqrt{(x_i - x_j)^2 + (y_i - y_j)^2}. \quad (5)$$

Since the piezoelectric elements of the phased-array ultrasound transducer are posed on concave spherical dome to be able to focus without the array of initial phase for excitation, the centers coordinates of the piezoelectric elements can be presented as

$$\begin{cases} x_i = R \sin \alpha_i \\ y_i = R(1 - \cos \alpha_i) \end{cases} \quad (6)$$

where  $R$  is the radius of the spherical surface of the phased-array ultrasound transducer and  $\alpha_i$  is the angle between the center axis of the spherical surface through center of the spherical dome surface and the line connected from the elements centers to the center of the spherical surface. The geometrical setup of the simulation is shown in Fig. 1 in which, the center of the spherical surface assigned as O, C is the center of the spherical dome.

For the pitch, the distances between each element in the concave phased-array ultrasound transducer can be expressed as

$$l = 2 \sin\left(\frac{\theta}{2}\right). \quad (7)$$

where the  $\theta = \frac{\alpha}{N-1}$  is the angle between each element viewed from the spherical surface center, calculated through the number of elements  $N$  and the angle of the spherical dome  $\alpha$  designed as the parameters of the phased-array ultrasound transducer.

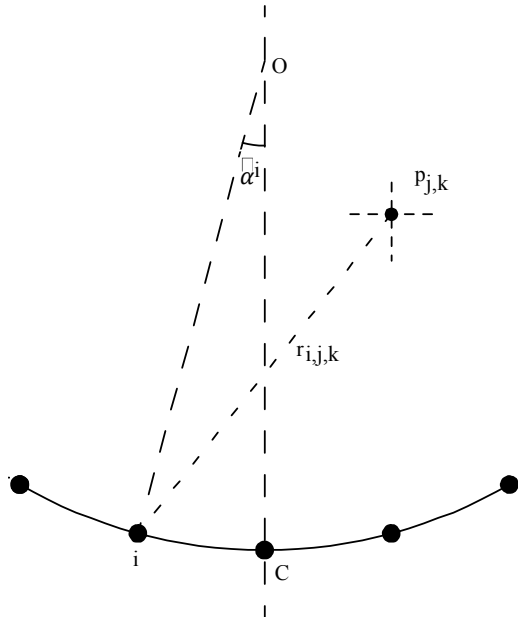


Fig. 1 The geometrical description of the numerical simulation circumstance in which the parameters were used to calculate the sound pressure amplitude at points of the perpendicular plane with the phased-array ultrasound transducer

Equation (2) requires the parameters of  $i, j, k$  specified the index of number of the phased-array ultrasound transducer element, and the coordinates of  $x$  and  $y$  in the perpendicular plane, respectively. Beside it, for the time variable, the numerical time array should be arranged. If  $q$  is the number of point of time in the calculation equation, (2) now can be rewritten numerically as

$$P_{i,j,k,q} = P_0 \sin(\omega t_q + k r_i(x_i, y_k)). \quad (8)$$

On the other hands, the wave number  $k$  presented as  $\frac{\omega}{c}$ , where  $c$  is the sound propagation speed in the acoustic media, hence (8) will be reduced to

$$P_{i,j,k,q} = P_0 \sin \left[ \omega \left( t_q + \frac{r_i(x_i, y_k)}{c} \right) \right]. \quad (9)$$

For the visualization of the ultrasound pressure field in the condition of varied frequencies and pitch to investigate the relationship between the frequencies and the pitch, the array of  $t_q$  should be presented through the number of cycles which related to the angular frequency. If the number of cycles assigned as  $T$ , the  $t_q$  can be expressed as

$$t_q = q \frac{T}{T_q} \frac{2\pi T_q}{\omega} = q 2\pi \frac{T}{\omega}. \quad (10)$$

where  $T_q$  is the interval time value.

The calculation of (9) under consideration of variation of time, elements, and points coordinates is sequential processes. For simplicity, to calculate the interfered sound pressures at the points in the perpendicular plane, this investigation were performed the computation by 4 four loops in which each loop present the variation of a parameter. The algorithm of the simulation is shown in Fig. 2.

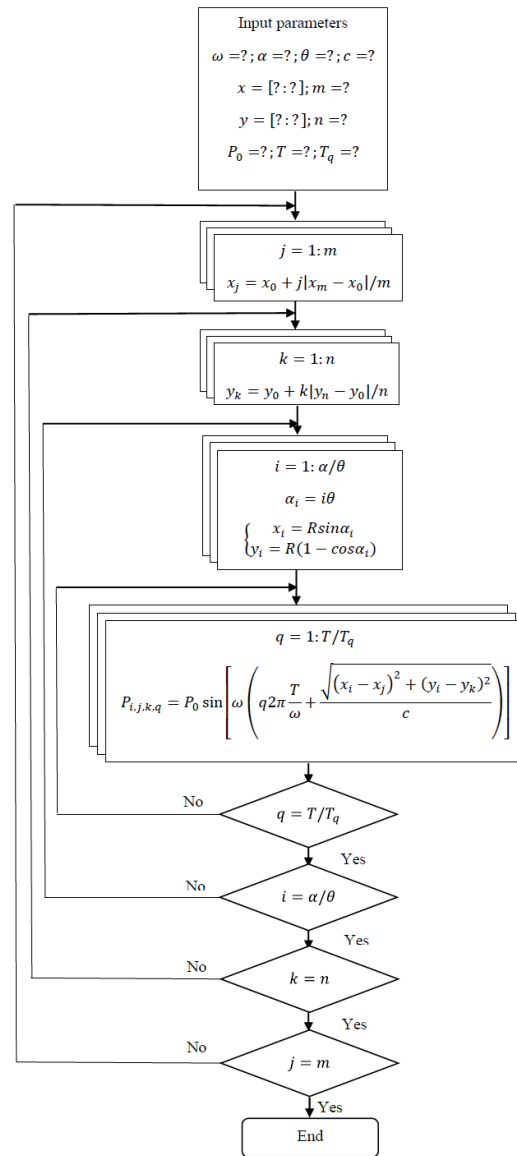


Fig. 2 The simulation algorithm for ultrasound pressure field visualization distributed in the perpendicular plane

The uniform distribution of the piezoelectric element in the spherical dome surface was represented by the arc as shown in Fig. 1 because of the computation cost in use of the for loops algorithm. For the input parameters such as  $\alpha$ ,  $R$ , and  $P_0$ , in this report, some model of commercial products were used to refer. The other parameters for the simulation can be set as conditions of the investigation to evaluate the ultrasound

pressure field pattern. The simulation was performed in Matlab environment.

The four loops in this simulated program returned a 4D array of calculated data as the result. For the visualization, the surface mesh function was used and it required a 2D array data. For this purpose, the data from the 4D array were extracted to be the 2D array data as the matrix whose elements values are ultrasound pressure amplitude at the points in the perpendicular plane. Through the variation of the pitch in condition of a certain frequency, the pattern of the ultrasound pressure field can be observed.

#### IV. RESULTS AND DISCUSSIONS

Fig. 1 shows the ultrasound pressure field pattern simulated in condition of 1MHz frequency corresponding to,  $\omega = 2\pi 10^6$  rad/s,  $\theta = 1^\circ$ ,  $R = 60$  mm,  $P_0 = 0.5$  kPa and  $\alpha = 30^\circ$ , where the x and y vector ranged on -30 to 30 mm and 30 to 90 mm with the parameters of  $m$  and  $n$  are 120, respectively. As the result shown, the maximum sound pressure amplitude located on the coordinate of  $p_{j,k} = (x_j = 0, y_k = 60)$  corresponding to the radius of the spherical surface dome. In this condition, there are no considerable side lobe beams are presented. Applying (7) to calculate the pitch length,  $l$  in this circumstance will be 0.02 mm approximately.

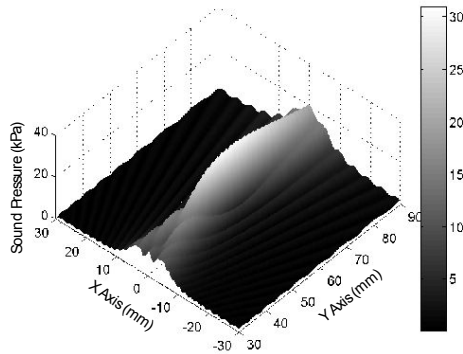


Fig. 3 Ultrasound pressure field simulated in condition of 1MHz frequency,  $\theta = 1^\circ$ ,  $R = 60$  mm,  $P_0 = 0.5$  kPa and  $\alpha = 30^\circ$

To examine the effects of pitch changes to the sound pressure field patterns,  $\theta$  was increased to  $2.5^\circ$  while the other conditions are fixed as constant. The pattern of the sound pressure field is shown in the Fig. 4. As the figure presented, there are 2 beams except of the straight beam appeared in the bottom corner of the figure. It means in the condition of pitch are 0.04 mm length approximately, the considerable side lobes are generated whose the angle viewed from the center of the spherical surface dome estimated in inverse tangent function as  $29^\circ$ .

To examine influences of the pitch changes to the angle of the side lobes appeared in the ultrasound pressure field pattern, the pitch lengths were increased to 0.06 mm approximately. The simulated result is shown in Fig. 5. As shown in the figure, the peaks of the side lobe beams are located on the coordinates of  $p_{j,k} = (x_j = 23, y_k = 53)$  and  $p_{j,k} =$

$(x_j = -23, y_k = -53)$ , respectively, where the side lobe angle reduced to  $24^\circ$  and the value of the ultrasound pressure peaks indicated as 8.5 kPa, lower than the perpendicular beam peak of 9 kPa.

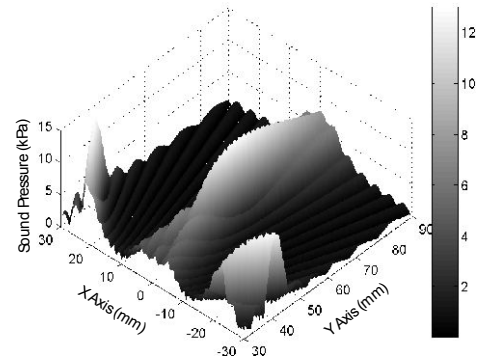


Fig. 4 Ultrasound pressure field simulated in condition of 1MHz frequency,  $\theta = 2.5^\circ$ ,  $R = 60$  mm,  $P_0 = 0.5$  kPa and  $\alpha = 30^\circ$

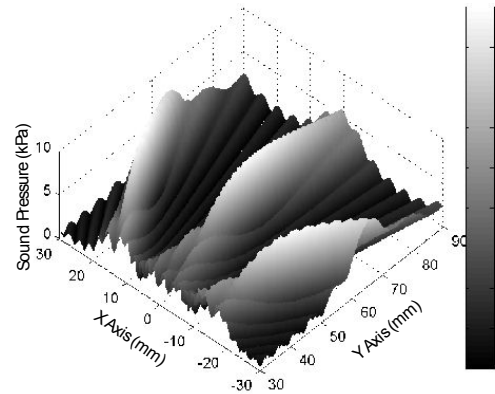


Fig. 5 Ultrasound pressure field simulated in condition of 1MHz frequency,  $\theta = 3.5^\circ$ ,  $R = 60$  mm,  $P_0 = 0.5$  kPa and  $\alpha = 30^\circ$

These results figured out that there are some effects of the pitch changes to the ultrasound pressure field pattern as the following responses: the side lobe beams peaks values are inverse proportional to the angles of the side lobe beams and proportional to the pitch lengths of the phased-array ultrasound transducer while the angle of the side lobe beam also inverse proportional to the pitch lengths. Consequently, since the modulated optical signal as well as the ultrasonic signal in biomedical imaging techniques depends on the ultrasound pressure field pattern, the ultrasound pressure strength of the side lobe beams might influence to the reliability of the reconstructed image with contamination of artifacts.

#### V. CONCLUSIONS

This paper reported a work of visualization for the ultrasound pressure field pattern generated from a phased-array ultrasound transducer in condition of varied pitch length. By the simple numerical method, the simulated program with the algorithm of for loops computation was established and

examined with a series of experiments to investigate the effects of pitch length change to the ultrasound pressure pattern. The results of the ultrasound pressure field pattern visualization with 3 different pitch lengths shows that the considerable side lobe beams presented when the pitch lengths of the phased-array ultrasound transducer are increased. Moreover, the values of the side lobe beams sound pressure peaks depends on the angle of the side lobe beams which inverse proportional to the pitch lengths of the phased-array ultrasound transducer. These results also explain the reason of the artifacts appeared on the reconstructed images obtained by the acousto-optic modulation technique in the condition of use of discontinuity element ultrasound transducers. Based on the preliminary numerical experiments, a parallel algorithm for computation which can reduce the computation cost, leading to the investigation close to the practical experiment condition will be developed in the future.

#### ACKNOWLEDGMENT

This works supported by Ministry of Education and Training through the project named as B2014-01-82 aiming to development a tool for focusing control to ultrasound beam.

#### REFERENCES

- [1] W. Leutz, and G. Maret, "Ultrasonic Modulation of Multiply Scattered-Light", *Physica B-Condensed Matter*, 204(1-4), 1995, pp.14-19.
- [2] M. Kobayashi, T. Mizumoto, Y. Shibuya, "Fluorescence tomography in turbid media based on acousto-optic modulation imaging," *Applied Physics Letters*, 89(18), 2006.
- [3] Grinvald A, Lieke E, Frostig RD, Gilbert CD, Wiesel TN, "Functional Architecture of Cortex revealed by optical imaging of intrinsic signals", *Nature* 324 (6095):1986, pp. 361 - 364
- [4] Hao F Zhang, Konstantin Maslov, George Stoica, Lihong V Wang, "Functional photoacoustic microscopy for high-resolution and noninvasive in vivo imaging", *Nature Biotechnology* 24, 2006, pp. 848 - 851.
- [5] S. Gunadi, and T. S. Leung, "Spatial sensitivity of acousto-optic and optical near-infrared spectroscopy sensing measurements," *Journal of Biomedical Optics*, 16(12), 127005-10, 2011.
- [6] Pu Wang, Justin R. Rajian, Ji-Xin Cheng, "Spectroscopic Imaging of Deep Tissue through Photoacoustic Detection of Molecular Vibration", *J.Phys.Chem.Lett*, 4, 2013, pp. 2177-2185.
- [7] K. Kirk Shung, Gary A. Thieme, "Ultrasonic Scattering in Biological Tissues", CRC Press, 1992.
- [8] Q. D. Trinh, Y. Nanbu, T. Suzuki, S. Takahashi, M. Takeda, M. Kobayashi, "Basic study on application of the phased-array transducer to determine fluorescence in turbid media based-on acousto-optic effects." *International Conference on Laser Applications in Life Sciences (LALS 2008)*.
- [9] Q. D. Trinh, Y. Nanbu, T. Suzuki, S. Takahashi, M. Takeda, M. Kobayashi, "Fluorescence tomography based-on acousto-optic modulations with phased-array ultrasound transducer." *BiOS Part of SPIE Photonic West*, paper No. 7177-57 (San Jose, USA, 2009).
- [10] T.Q.Duc, S.Kaneta, M.Masaki, "Development of Ultrasonic Modulation Probe for Fluorescence Tomography Based on Acousto-Optic Effect." *International Journal Optic*, Vol. 2011, 818302, pp. 1-6.
- [11] T. Q. Duc, S. Kaneta, M. Kobayashi, "Study on the Mechanism of Ultrasonic Fluorescence Modulation in Light Scattering Medium Based on Diffusion Approximation with Varying Refractive Index." *Optical Review* Vol. 19, No. 3, 2012, pp. 1-8.
- [12] André LAMARRE, "Dynamic Focusing of Phased Arrays for Nondestructive Testing: Characterization and Application", *NDT.net*, Vol. 4 No. 9, 1999.